LLNL-PROC-539171

LAWRENCE
LIVERMORE
NATIONAL
LABORATORY

Ultra Low Density Amorphous Shape Memory polymer Foams.

P. Singhal, W. Small, J. N. Rodriguez, S. Letts, D. J. Maitland, T. S. Wilson

March 19, 2012

American Chemical Society
Philadelphia, PA, United States
August 19, 2012 through August 23, 2012

Disclaimer

This document was prepared as an account of work sponsored by an agency of the United States government. Neither the United States government nor Lawrence Livermore National Security, LLC, nor any of their employees makes any warranty, expressed or implied, or assumes any legal liability or responsibility for the accuracy, completeness, or usefulness of any information, apparatus, product, or process disclosed, or represents that its use would not infringe privately owned rights. Reference herein to any specific commercial product, process, or service by trade name, trademark, manufacturer, or otherwise does not necessarily constitute or imply its endorsement, recommendation, or favoring by the United States government or Lawrence Livermore National Security, LLC. The views and opinions of authors expressed herein do not necessarily state or reflect those of the United States government or Lawrence Livermore National Security, LLC, and shall not be used for advertising or product endorsement purposes.

ULTRA LOW DENSITY AMORPHOUS SHAPE MEMORY POLYMER FOAMS

Pooja Singhal [1,2], Ward Small [2], Jennifer N. Rodriguez [1], Steve Letts [2],
Duncan J. Maitland [1,2] and Thomas S. Wilson [2]

[1] Department of Biomedical Engineering,
Texas A&M University,
College Station, TX-77843

[2] Physical and Life Sciences Directorate,
Lawrence Livermore National Laboratory,
Livermore, CA-94550

Introduction

Thermally actuated shape memory polymers (SMPs) are a class of smart materials that have gained significant interest in recent years. These materials are capable of remembering two shapes (a primary shape, and another secondary or deformed shape), and they can be actuated from one shape to the other by application of an appropriate thermal stimulus. Multiple reviews and applications of these shape memory polymers are available in the literature.[1-2] In porous form, as SMP foams, these materials have additional biomedical applications, such as tissue regeneration scaffolds and embolic devices for treatment of aneurysms.[3-4]

Our group is interested in developing foam based embolic SMP devices that can be delivered to a target location in the body, such as an aneurysm, via a minimally invasive catheterization process.[4-6] One proposed strategy is to heat a spherical foam sample above its actuation temperature (*Tg*) and compress it to a rod like secondary shape. This secondary shape is fixed by cooling the compressed sample to below its *Tg*. The rod-shaped device can then be delivered to the aneurysm site via a catheterization process, in a minimally invasive clinical procedure. Once the device reaches its target site, it can be actuated to its primary spherical shape by heating it up to its *Tg*, thus embolizing the aneursym.

A material that may be used for this application needs to have two main properties – a) very low density that can allow deformation of the device to a small enough dimension that is deliverable via a catheter, and b) a high modulus that allows shape recovery against the physiological media even at these low densities. Also the shape memory needs to be stable, limiting the secondary shape forming typically seen in some other commercially available SMP foams.[7] Novel foams based on materials proposed by Wilson et al.[8] with small molecular weight monomers and highly chemically crosslinked network structure, were developed to achieve these design goals (**Figure 1(a)**).[4] Here we report the synthesis of these novel materials and some key physical properties demonstrating their potential utility in biomedical applications.

Experimental

Materials. Monomers 2,2',2''-Nitrilotriethanol (TEA, 98%, Alfa Aesar Inc.), N,N,N‘,N‘-Tetrakis(2-hydroxypropyl) ethylenediamine (HPED, 99%, Sigma Aldrich Inc.) and 1,6-Diisocyanatohexane (HDI, TCI America Inc) were used as received for the foam synthesis. The foams were synthesized in a three step process.[4] First, a prepolymer with excess isocyanate was prepared by adding 38 hydroxyl equivalents to 100 isocyanate equivalents, and allowed to cure for two days. Secondly, a hydroxyl premix was prepared by mixing all the remaining hydroxyl monomers (maintaining a 105 isocyanate index) with the chemical blowing agent (DI water) and surfactants and catalysts (Air Products Inc.). Lastly, the foams were synthesized by mixing calculated amounts of isocyanate and hydroxyl premixes along with the physical blowing agent Enovate, HFC 245-fa (Honeywell Corp.). Foams were allowed to cure for at least a week before further characterization (**Table 1**).

Density and cell structure. Density of the foams was calculated from the top, middle and bottom sections using the ASTM standard D-3574-08. For capturing the images, thin slices (1-2 mm in thickness) of foams were cut and imaged using the Leica MZ8 microscope (Leica Microsystems Inc.) with RSImage Software (Roper Scientific Inc.) in the brightfield mode as described by Singhal et al.[4]

Table 1: Composition of the foams in terms of wt% of constituents in the net formulation.

Chemical name	Wt%
HDI	63.85
HPED	15.67
TEA	9.40
Water	2.86
Surfactants DC5179 and DCI990	7.29
Catalysts T131 and BL22	0.92
Enovate (pph) 7.80	

Differential scanning calorimetry (DSC). *Tg* was measured using a Pyris Diamond DSC (Perkin Elmer Inc.). A vented aluminum pan loaded with a 3-5 mg sample was cooled to -40 C. Thereafter, a heat - cool - heat cycle was run from -40 to 120 C. *Tg* was estimated from the half height of transition during the second heating cycle.

Fourier transform infrared spectroscopy (FTIR). An FTIR spectrum of the foam was collected using the Spectrum 2000 FTIR (Perkin Elmer Inc.). The sample chamber was purged with nitrogen gas for 5 minutes and a background spectrum was captured. Thereafter, thin slices of foams were cut and placed on a 2 cm^{-1} JStop holder (0.88 cm aperture). The chamber was again purged for 5 minutes after placing the sample, and an FTIR spectrum was collected in the transmission mode at a resolution of 4 cm^{-1}. The test was performed in duplicate to ascertain reproducibility of spectra. A total of 50 scans were taken for each sample and the background spectrum was subtracted using the Spectrum software (Perkin Elmer Inc.).

Shape memory behavior. For quantifying the shape recovery of the foams, constrained stress recovery tests were performed in an ARES-LS2 rheometer (TA Instruments) according to a previously described method.[4] Tests were performed in a compressive mode using parallel plate fixtures on cylindrical foam samples, approximately 15 mm high and 20 mm in diameter. The sample was first heated to a temperature of 100 C (*Tg*+30 C) and deformed to 80% compressive strain at a rate of 2.5 mm min^{-1}. Thereafter the sample was cooled to 40 C (*Tg*-30 C) and then heated back up to 100 C (*Tg*+30 C) maintaining the 80% strain. At the end of the cool-heat cycle, the strain was released at a rate of 2.5 mm min^{-1} and the recovered strain was measured from the distance between the plates at a 10 g axial force. Three samples were tested and five cycles were performed on each of the samples.

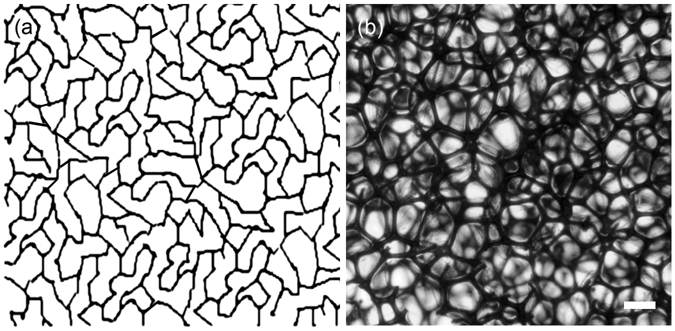

Figure 1: (a) Schematic representation of the polymer network structure of the foams showing low molecular weight between covalently bonded network points. **(b)** Macroscopic structure of the foams as seen from an optical microscope (scale bar = 400 um).

Volume expansion. A SC150-42 Stent Crimper (Machine Solutions Inc.) was used to measure the maximum volume expansion of foam.[4] 6-mm-diameter cylindrical foam samples were loaded in the crimper and compressed as small as possible, at 100 C (~*Tg*+30 C). The compressed shape was fixed by allowing them to cool down to room temperature in the constrained state. The compressed diameter was measured using a digital micrometer. Finally, the samples were heated back to 100 C (~*Tg*+30 C) in air, and the recovered diameter was measured. Any change in length was ignored and the net volume expansion was calculated as $\left(\frac{Recovered\ Diameter}{Compressed\ Diameter}\right)^2$.

Results and Discussion

Density and cell Structure. An average density of foams was found to be 0.018±.001 g/cc. With a neat polymer density of approximately 1.17 g/cc, this corresponds to a theoretical porosity of ~98%.

The cell structure of the foams is shown in **Figure 1(b)**. A mixed open to closed cell structure is seen, with thin residual membranes on the cell surface as reported by Singhal et al. [4]

Differential scanning calorimetry. DSC of the sample gave a sharp, single *Tg* at 67 C. This composition uses 2:1 ratio of hydroxyls from HPED vs. TEA, as compared to 3:2 ratio of hydroxyls from HPED vs. TEA of a composition reported previously.[4] A higher HPED content may explain a slightly higher *Tg* of these foams compared to the previously reported foams.[4]

Fourier transform infrared spectrocopy. An FTIR spectrum of the foam is shown in **Figure 2**. As reported previously for similar compositions of foams [4] a shoulder in the urethane peak was observed indicating the presence of urea groups. The position of the C=O peak has been reported in the FTIR spectra of polyurethanes. For hydrogen bonded urethane it has been reported at 1703-1710 cm^{-1} [9], 1694 cm^{-1} [10] and 1706-1713 cm^{-1} [11]. For free urethane it has been reported at 1730-1740 cm^{-1} [9], 1729-1739 cm^{-1} [11] and 1725 cm^{-1} [10]. The shift of the urethane peak to a low wavenumber (~1694 cm^{-1}) here suggests the presence of a high degree of hydrogen bonding in these materials.

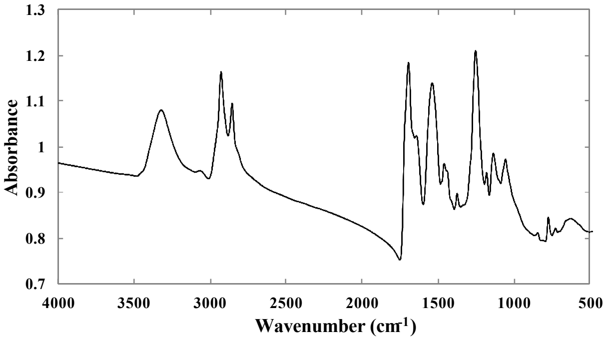

Figure 2. FTIR spectrum of the foam.

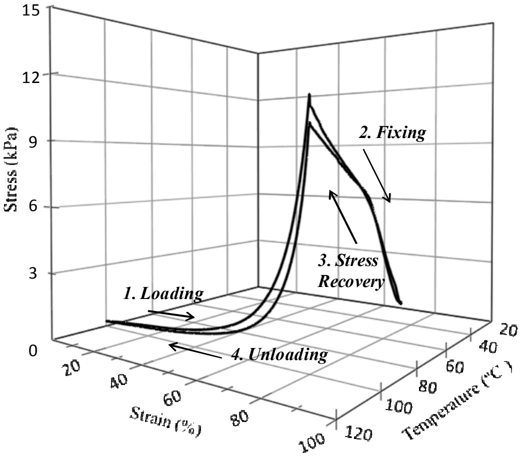

Figure 3. Constrained stress recovery of the foam samples. Variation in the stress, strain and temperature profiles of the foam sample is demonstrated during the loading, fixing, stress recovery and unloading stages of the shape memory cycle.

Shape memory behavior. Four key steps comprising the typical shape memory response are depicted in **Figure 3**. **1)** ***Loading*** refers to the deformation of the foam sample to 80% compressive strain at a temperature above its actuation temperature (*Tg*+30 C). **2)** ***Fixing*** refers to cooling the compressed sample below its actuation temperature (*Tg*-30 C) while maintaining the 80% strain, thereby fixing the deformed shape. **3)** ***Stress recovery*** involves heating the sample up to *Tg*+30 C while maintaining its compressed state. A concomitant increase in stress is noticed as the sample tries to recover its primary shape with the increase in temperature. Finally, **4)** ***unloading*** refers to removal of the strain and recovery of the sample to its primary shape at *Tg*+30 C. The initial two cycles showed a relatively higher hysteresis with an average of 90% and 92% shape recovery. After this initial conditioning, a higher average shape recovery of 97% was achieved.

Volume expansion. An average volume expansion of approximately 70 times was seen for these foams. **Figure 4** shows the expansion of a compressed foam device in a heated water bath. Almost immediate actuation of the foam is noticed on exposure to the water bath.

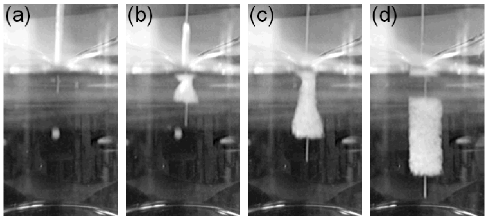

Figure 4. Actuation of shape memory polymer foams in a water bath heated to *Tg*.

Conclusions

This work reports polyurethane based novel shape memory polymer foams. These materials are designed to have a highly chemically crosslinked network structure by usage of low molecular weight multifunctional hydroxyl monomers. Ultra low densities of ~0.018 g cm^{-3} were achieved in these foams and a mixed, open to closed, cell morphology was noticed with thin residual membranes on the cell surfaces. FTIR results suggested strong hydrogen bonding in the material. Post initial conditioning cycles, excellent shape recovery of up to 97% was recorded, and a 70 times volume expansion was seen with near immediate actuation of the device on exposure to water at *Tg*. With these unique properties, these materials are expected to be particularly promising as biomaterials for embolic devices in minimally invasive medical applications.

Acknowledgements

This work was partially performed under the auspices of the U.S. Department of Energy by Lawrence Livermore National Laboratory under Contract DE-AC52-07NA27344 and supported by the National Institutes of Health/National Institute of Biomedical Imaging and Bioengineering Grant R01EB000462 and by Lawrence Livermore National Laboratory Directed Research and Development (LDRD) Grants 04-LW-054 and 04-ERD-093.

References

(1) Liu, C.; Qin, H.; Mather, P. *Journal of Materials Chemistry* **2007**, *17*, 1543.
(2) Mather, P. T.; Luo, X.; Rousseau, I. A. *Annual Review of Materials Research* **2009**, *39*, 445.
(3) Sokolowski, W.; Metcalfe, A.; Hayashi, S.; Yahia, L. H.; Raymond, J. *Biomedical Materials* **2007**, *2*, S23.
(4) Singhal, P.; Rodriguez, J. N.; Small, W.; Eagleston, S.; Van de Water, J.; Maitland, D. J.; Wilson, T. S. *Journal of Polymer Science: Part B: Polymer Physics* **2012**, DOI: 10.1002/polb.23056.
(5) Maitland, D. J.; Small IV, W.; Ortega, J. M.; Buckley, P. R.; Rodriguez, J.; Hartman, J.; Wilson, T. S. *Journal of Biomedical Optics* **2007**, *12*, 030504.
(6) Small, W.; Buckley, P.; Wilson, T. S.; Benett, W. J.; Hartman, J.; Saloner, D.; Maitland, D. J. *Biomedical Engineering, IEEE Transactions on* **2007**, *54*, 1157.
(7) Tobushi, H.; Matsui, R.; Hayashi, S.; Shimada, D. *Smart Materials and Structures* **2004**, *13*, 881.
(8) Wilson, T.; Bearinger, J.; Herberg, J.; Marion III, J.; Wright, W.; Evans, C.; Maitland, D. *Journal of Applied Polymer Science* **2007**, *106*, 540.
(9) Yılgör, E.; Yılgör, İ.; Yurtsever, E. *Polymer* **2002**, *43*, 6551.
(10) Zhang, L.; Jeon, H. K.; Malsam, J.; Herrington, R.; Macosko, C. W. *Polymer* **2007**, *48*, 6656.
(11) Ning, L.; De-Ning, W.; Sheng-Kang, Y. *Macromolecules* **1997**, *30*, 4405.